AD_____

Award Number: DAMD17-98-1-8298

TITLE: Mechanisms for Breast Cancer Cell Resistance to
       Doxorubicin and Solutions to Resistance and Side Effects

PRINCIPAL INVESTIGATOR: Tad H. Koch, Ph.D.

CONTRACTING ORGANIZATION: University of Colorado
                          Boulder, Colorado 80309-0019

REPORT DATE: October 2000

TYPE OF REPORT: Annual

PREPARED FOR: U.S. Army Medical Research and Materiel Command
               Fort Detrick, Maryland 21702-5012

DISTRIBUTION STATEMENT: Approved for Public Release;
                        Distribution Unlimited

The views, opinions and/or findings contained in this report are
those of the author(s) and should not be construed as an official
Department of the Army position, policy or decision unless so
designated by other documentation.

1

REPORT DOCUMENTATION PAGE

Public reporting burden for this collection of information is estimated to average 1 hour per response, including the time for reviewing instructions, searching existing data sources, gathering and maintaining the data needed, and completing and reviewing this collection of information. Send comments regarding this burden estimate or any other aspect of this collection of information, including suggestions for reducing this burden to Washington Headquarters Services, Directorate for Information Operations and Reports, 1215 Jefferson Davis Highway, Suite 1204, Arlington, VA 22202-4302, and to the Office of Management and Budget, Paperwork Reduction Project (0704-0188), Washington, DC 20503

1. AGENCY USE ONLY (Leave blank)	2. REPORT DATE October 2000	3. REPORT TYPE AND DATES COVERED Annual (15 Sep 99 - 14 Sep 00)

4. TITLE AND SUBTITLE	5. FUNDING NUMBERS
Mechanisms for Breast Cancer Cell Resistance to Doxorubicin and Solutions to Resistance and Side Effects	DAMD17-98-1-8298

6. AUTHOR(S)
Tad H. Koch, Ph.D.

7. PERFORMING ORGANIZATION NAME(S) AND ADDRESS(ES)	8. PERFORMING ORGANIZATION REPORT NUMBER
University of Colorado Boulder, Colorado 80309-0019 E-MAIL: tad.koch@colorado.edu	

9. SPONSORING / MONITORING AGENCY NAME(S) AND ADDRESS(ES)	10. SPONSORING / MONITORING AGENCY REPORT NUMBER
U.S. Army Medical Research and Materiel Command Fort Detrick, Maryland 21702-5012	

11. SUPPLEMENTARY NOTES
This report contains colored photos

12a. DISTRIBUTION / AVAILABILITY STATEMENT Approved for public release; distribution unlimited	12b. DISTRIBUTION CODE

13. ABSTRACT (Maximum 200 Words)

The anthracyclines, doxorubicin and epidoxorubicin, continue to be important drugs for the treatment of breast cancer. Recent studies refocus attention to anthracycline-alkylation and crosslinking of DNA as important toxic events triggering cell death. The long term goals of the proposed research are to establish the mechanism for the crosslinking, to produce new mechanism-based anthracycline derivatives which will be active against resistant breast cancer, and to develop a delivery vehicles for the improved drugs. New derivatives have been synthesized and characterized as the formaldehyde conjugates of doxorubicin and epidoxorubicin, doxoform and epidoxoform, respectively. The following results were obtained during the current year: 1) Sensitive but not resistant breast cancer cells show anthracycline induction of formaldehyde synthesis. 2) Apoptosis assays of drug-treated cells show similar patterns for doxorubicin and doxoform consistent with doxoform being a prodrug to the doxorubicin active metabolite. 3) Epidoxoform shows broad spectrum toxicity to human cancer cells including resistant cancer cells. 4) Epidoxoform can be formulated in DMSO/Cremaphor as a drug delivery vehicle. The new results continue to support a mechanism for drug toxicity which utilizes drug-induced formaldehyde synthesis and support epidoxoform as a new compound for the treatment of resistant breast cancer.

14. SUBJECT TERMS Breast Cancer			15. NUMBER OF PAGES 17
			16. PRICE CODE

17. SECURITY CLASSIFICATION OF REPORT Unclassified	18. SECURITY CLASSIFICATION OF THIS PAGE Unclassified	19. SECURITY CLASSIFICATION OF ABSTRACT Unclassified	20. LIMITATION OF ABSTRACT Unlimited

NSN 7540-01-280-5500

Standard Form 298 (Rev. 2-89)
Prescribed by ANSI Std. Z39-18
298-102

Table of Contents

(4) INTRODUCTION

Preliminary experiments with deoxyoligonucleotides indicated that the anthracycline antitumor drug, doxorubicin, covalently bonds to DNA through its catalysis of formaldehyde production (1-3). Subsequently, it utilizes formaldehyde for covalent attachment to DNA from its 3'-amino group to the 2-amino group of a G-base (4-6). At a 3'-GC-5' site the combination of drug intercalation, covalent bonding to one strand and hydrogen bonding to the other strand serves to virtually crosslink the DNA (7). This mechanistic understanding prompted the synthesis of anthracycline formaldehyde conjugates as improved antitumor drugs (8, 9). The first conjugate synthesized, doxoform, proved to be highly toxic to sensitive and resistant breast cancer cells; however, doxoform rapidly hydrolyzes to doxorubicin under physiological conditions (8). The purpose and scope of the research are to design and synthesize a hydrolytically more stable anthracycline-formaldehyde conjugate, to establish that anthracyclines derive at least some of their toxicity to tumor cells from covalent bonding to DNA, to determine why anthracycline-formaldehyde conjugates overcome at least some resistance mechanisms, and to a develop drug delivery vehicle for anthracycline-formaldehyde conjugates.

(5) BODY

Research Accomplishments

During the current grant period the following questions were addressed:

What is the abundance of formaldehyde in sensitive tumor cells, resistant tumor cells and/or non-malignant cells with and without addition of daunorubicin or doxorubicin? The abundance of formaldehyde in sensitive MCF-7 and resistant MCF-7/Adr cells was measured using selected ion flow tube mass spectrometry (10). No formaldehyde above background levels was observed in the media containing growing, sensitive or resistant cells with or without drug treatment. Drug treated sensitive cells, but not resistant cells, showed formaldehyde levels above background when lysed. A lower limit for excess formaldehyde in MCF-7 cells treated with 0.5 μM daunorubicin for 24 h is 0.3 mM. This result supports a mechanism for drug cytotoxicity which involves drug induction of metabolic processes leading to formaldehyde production followed by drug utilization of formaldehyde to virtually cross-link DNA.

Does doxoform cause tumor cell death by apoptosis. Three different apoptosis assays were used to compare doxorubicin and doxoform with respect to induction of programmed cell death. The assays were formation of a DNA ladder, the TUNNEL assay, and annexin V/propidium iodide staining. The assays were performed with Hela S_3, MCF-7 and MCF-7/Adr cells. Doxoform was used at 10-fold lower dose because of the 10-fold higher cytotoxicity of doxoform. At these relative doses doxorubicin and doxoform gave the same response with all three cell lines: apoptotic death of Hela S_3 cells and non-apoptotic death of MCF-7 and MCF-7/Adr cells. This result supports the hypothesis that doxoform is a prodrug to the active metabolite of doxorubicin.

How does epidoxoform compare with epidoxorubicin and doxorubicin in the NCI tumor cell screen? Epidoxoform (EPIF) was submitted to the National Cancer Institute Developmental Therapeutics Program for screening in their 60 human tumor cell assay. The log of the concentration of drug which inhibited 50% of the growth is compared in Table 1 with values for doxorubicin (DOX) and epidoxorubicin (EPI). Values which measure tumor cell resistance mechanisms, rhodamine efflux, multidrug resistance gene (mdr-1), multidrug resistance protein (MRP), and lung resistance protein (LRP), are compared for some cell lines. The mean values for the three drugs show that epidoxoform is approximately 0.5 log more cytotoxic than doxorubicin and 1 log more cytotoxic than epidoxorubicin. Further, epidoxoform is active against cells which express all three resistance proteins: MDR, MRP, and LRP.

4

Table 1. National Cancer Institute (NCI) In-Vitro Human Tumor Cell Screen and Tumor Cell Resistance Parameters

Panel/Cell Line	log GI50 (M)			rhodamine[d] efflux	mdr-1[d]	MRP[d]	LRP[d]
	EPIF[a]	DOX[b]	EPI[c]				
Leukemia							
CCRF-CEM	-8.52	-7.46	-7.35	35	0.4	1.2	0.0
HTL-60 (TB)	-8.57	-7.29	-7.24				
MOLT-4	-8.60	-7.96	-7.77				
RPMI-8226	-8.31	-7.35	-7.26				
Non Small Cell Lung Carcinoma (NSCLC)							
A549/ATCC	-7.89	-7.14	-7.10				
EKVX	-7.07	-6.17	-6.52				
HOP-62	-7.66	-7.30	-6.82	62	3.4	1.3	1.7
HOP-92	-7.82	-7.09	-6.51				
NCI-H226	-7.44	-7.29	-7.36				
NCI-H23	-7.92	-6.96	-7.12				
NCI-H322M	-7.55	-6.31	-6.04				
NCI-H460	-8.35	-8.33	-7.60				
NCI-H522	-8.17	-7.22	-6.72				
Colon Cancer							
COLO 205	-7.90	-6.67	-6.30				
HCC-2998	-7.12	-6.63	-6.51	-5	0.1	1.1	2.0
HCT-116	-7.78	-7.18	-7.17	26	5.8	1.8	2.5
HCT-15	-6.93	-5.88	-5.41	414	457	1.6	0.1
HT29	-7.70	-6.73	-6.51				
KM12	-7.34	-6.56	-6.43				
SW-620	-7.98	-7.12	-6.91	31	19.4	0.8	0.3
Central Nervous System Cancer							
SF-268	-8.20	-6.96	-6.66				
SF-295	-7.51	-7.04	-6.68	91	8.3	1.6	0.8
SF-539	-8.26	-7.16	-6.71				
SNB-19	-7.82	-7.31	-7.04				
SNB-75	-8.12	-7.04	-6.60				
U251	-8.11	-7.39	-7.07	-19	2.7	1.1	0.1
Melanoma							
MALME-3M	-7.80	-7.16	-6.85				
M14	-7.30	-6.66	-6.37				
SK-MEL-2	-7.64	-6.63	-6.70	11	2.8	0.8	0.1
SK-MEL-28	-7.31	-6.56	-6.23				
SK-MEL-5	-7.35	-7.17	-6.95	12	13	2.3	1.6
UACC-257	-7.28	-6.66	-6.47				
UACC-62	-8.30	-7.19	-6.82				
Ovarian Cancer							
IGROV1	-7.76	-6.87	-6.57				
OVCAR-3	-7.33	-6.40	-6.33				
OVCAR-4	-6.98	-6.19	-5.92	-4	0.1	2.0	1.0
OVCAR-5	-7.05	-6.28	-6.14				

OVCAR-8	-7.75	-6.88	-6.70				
SK-OV-3	-6.88	-6.66	-6.39				

Renal Cancer

786-0	-8.10	-7.31	-7.00	-44	18.4	0.5	1.5
A498	-8.42	-6.98	-	108	71	-	-
ACHN	-8.09	-7.21	-6.57	120	31	0.0	1.5
CAKI-1	-7.76	-6.77	-6.57	171	177	0.4	2.3
SN12C	-7.80	-7.04	-6.77	-86	2.2	0.4	1.5
TK-10	-6.63	-6.39	-6.14				
UO-31	-6.84	-6.13	-5.72	244	749	1.8	2.4

Prostate Cancer

PC-3	-7.30	-6.70	-6.62
DU-145	-7.92	-6.83	-6.57

Breast Cancer

MCF-7/ADR-RES	-6.49	-4.78	-
MDA-MB-231/ATCC	-7.32	-6.41	-6.02
HS-578T	-7.21	-6.71	-8.00
MDA-MB-435	-7.19	-6.51	-6.21
MDA-N	-7.28	-6.58	-6.86
BT-549	-6.93	-6.62	-6.36
T-47D	-7.16	-7.04	-7.03

Mean

	-7.64	**-6.87**	**-6.70**

[a]Single determination with log maximum concentration (M) = -4.6.

[b]Average of multiple determinations with log maximum concentration (M) = -4.6.

[c]Single determination with log maximum concentration (M) = -4.0.

[d]Values obtained from the NCI Developmental Therapeutics Program web site: http://dtp.nci.nih.gov/; MRP (multidrug resistant protein), LRP, lung resistant protein.

Why is doxorubicin more cytotoxic than epidoxorubicin, and doxoform more cytotoxic than epidoxoform? An important cytotoxicity factor appears to be the rate of release of drug from the nucleus. This was measured for drug release from MCF-7/Adr cells by flow cytometry using drug fluorescence as a measure of drug in cells. MCF-7/Adr cells overexpress P-170 efflux pump and hence will excrete drug as soon as it is released from the nucleus by hydrolysis of drug DNA covalent adducts and drug DNA virtual crosslinks. The kinetics were fit to a biexponential rate law consistent with the kinetics of release of drug from DNA (1, 11). With doxorubicin and doxoform the half-life for the more rapid release was 2 h and for the slow release 29 h and with epidoxorubicin and epidoxoform, 4 h and 13 h, respectively. The important factor is likely the slow component of release which is proposed to result from hydrolysis of drug-DNA virtual crosslinks.

Can doxoform and epidoxoform be stabilized with respect to hydrolysis in a liposome as a drug delivery vehicle? The stability of both doxoform and epidoxoform was measured in several drug delivery vehicles: mono lamellar liposomes, multi lamellar liposomes, and surfactants. The drug delivery vehicle which gave the best stabilization with respect to hydrolysis and dissolved the most drug was DMSO/Cremaphor EL. When a solution of epidoxoform in 40% DMSO / 60% Cremaphor EL was added to a pH 7.4 buffer at 37 °C, no precipitation of drug occurred and only a trace amount of hydrolysis to epidoxorubicin was observed even after 90 min. Both liposomal delivery systems were less effective primarily because they dissolved much less drug.

(6) KEY RESEARCH ACCOMPLISHMENTS:

Doxorubicin and daunorubicin induce production of formaldehyde in sensitive breast cancer cells but not in resistant breast cancer cells.

Doxoform at 10-fold lower dose functions the same as doxorubicin with respect to induction of apoptosis.

Epidoxoform inhibits the growth of 60 human tumor cell lines 0.5 log better than doxorubicin and 1 log better than epidoxorubicin.

Higher toxicity of doxorubicin relative to epidoxorubicin correlates with a longer half-life for the respective drug-DNA virtual crosslink.

A promising drug delivery vehicle for epidoxoform is 40% DMSO/ 60% Cremaphor EL.

(7) REPORTABLE OUTCOMES:

- manuscripts

Podell, E. R.; Harrington, D. J.; Taatjes, D. J.; Koch, T. H. "Crystal Structure of Epidoxoform-formaldehyde *Virtual Crosslink* of DNA and Evidence for Its Formation in Human Breast Cancer Cells" *Acta Cryst., D55*, 1516-1523 (1999).

Taatjes, D. J.; Koch, T. H. "Nuclear Targeting and Retention of Anthracycline Antitumor Drugs in Sensitive and Resistant Tumor Cells" *Curr. Med. Chem., 7,* in press (2000).

Dernell, W. S.; Powers, B. E.; Taatjes, D. J.; Cogan, P.; Gaudiano, G.; Koch, T. H. "Evaluation of the Epidoxorubicin-formaldehyde Conjugate, Epidoxoform, in a Mouse Mammary Carcinoma Model" *Cancer Invest.*, submitted (2000).

- abstracts

"Nuclear Targeting and Nuclear Retention of Anthracycline-formaldehyde conjugates", T. H. Koch, D. J. Taatjes, D. J. Fenick, Era Of Hope Meeting, Atlanta, GA, June 2000.

- presentations

"Nuclear Targeting and Nuclear Retention of Anthracycline-formaldehyde conjugates", T. H. Koch, D. J. Taatjes, D. J. Fenick, Era Of Hope Meeting, Atlanta, GA, June 2000.

"Cytotoxic Mechanism for Anthracycline Antitumor Drugs and New Anthracycline-formaldehyde Conjugates Toxic to Resistant Cancer Cells", T. H. Koch, D. J. Taatjes, D. J. Fenick, S. Kato, P. J. Burke, V. Bierbaum, P. Cogan, E. R. Podell, D. J. Harrington, CU Roche Symposium on Synthetic Chemistry, May 2000.

- degrees

Catherine Fowler, M.S. degree with thesis.

(8) CONCLUSIONS

The results from the current year's experiments provide additional support for the hypothesis that the anthracycline antitumor drugs derive at least some of their toxicity from induction of formaldehyde

synthesis and use of formaldehyde for drug-covalent bonding to DNA. Sensitive but not resistant breast cancer cells show anthracycline induction of formaldehyde synthesis. Apoptosis assays show similar patterns with doxorubicin and doxoform. Relative cytotoxicity of doxorubicin and epidoxorubicin correlates with the rate of drug release from resistant cells which parallels the rate of hydrolysis of drug-DNA virtual crosslinks. At least some resistance to anthracyclines stems from resistance to drug induction of formaldehyde synthesis. Anthracycline-formaldehyde conjugates overcome resistance mechanisms associated with inhibition of formaldehyde synthesis and expression of MDR, MRP and LRP resistance proteins and are prodrugs of anthracycline active metabolites. Epidoxoform can be formulated in DMSO/Cremaphor as a drug delivery vehicle.

(9) REFERENCES

(1) Cullinane, C., van Rosmalen, A. and Phillips, D. R. (1994) Does adriamycin induce interstrand cross-links in DNA? *Biochemistry* 33, 4632-4638.

(2) Taatjes, D. J., Gaudiano, G., Resing, K. and Koch, T. H. (1996) Alkylation of DNA by the Anthracycline, Antitumor Drugs Adriamycin and Daunomycin. *J. Med. Chem.* 39, 4135-4138.

(3) Taatjes, D. J., Gaudiano, G. and Koch, T. H. (1997) Production of formaldehyde and DNA-adriamycin or -daunomycin adducts, initiated through redox chemistry of DTT/iron, xanthine oxidase/NADH/iron, or glutathione/iron. *Chem. Res. Toxicol.* 10, 953-961.

(4) Wang, A. H. J., Gao, Y. G., Liaw, Y. C. and Li, Y. K. (1991) Formaldehyde cross-links daunorubicin and DNA efficiently: HPLC and X-ray diffraction studies. *Biochemistry* 30, 3812-3815.

(5) Zeman, S. M., Phillips, D. R. and Crothers, D. M. (1998) Characterization of covalent adriamycin-DNA adducts. *Proc. Natl. Acad. Sci. USA* 95, 11561-11565.

(6) Podell, E. R., Harrington, D. J., Taatjes, D. J. and Koch, T. H. (1999) Crystal structure of epidoxorubicin-formaldehyde virtual crosslink of DNA and evidence for its formation in human breast-cancer cells. *Acta Cryst.* D55, 1516-1523.

(7) Taatjes, D. J., Gaudiano, G., Resing, K. and Koch, T. H. (1997) A redox pathway leading to the alkylation of DNA by the anthracycline, anti-tumor drugs, adriamycin and daunomycin. *J. Med. Chem.* 40, 1276-1286.

(8) Fenick, D. J., Taatjes, D. J. and Koch, T. H. (1997) Doxoform and Daunoform: anthracycline-formaldehyde conjugates toxic to resistant tumor cells. *J. Med. Chem.* 40, 2452-2461.

(9) Taatjes, D. J., Fenick, D. J. and Koch, T. H. (1998) Epidoxoform: a hydrolytically more stable anthracycline-formaldehyde conjugate, cytotoxic to resistant tumor cells. *J. Med. Chem.* 41, 1306-1314.

(10) Kato, S., Burke, P. J., Fenick, D. J., Taatjes, D. J., Bierbaum, V. M. and Koch, T. H. (2000) Mass spectrometric measurement of formaldehyde generated in breast cancer cells upon treatment with anthracycline antitumor drugs. *Chem. Res. Toxicol.* 13, 509-516.

(11) van Rosmalen, A., Cullinane, C., Cutts, S. M. and Phillips, D. R. (1995) Stability of adriamycin-induced DNA adducts and interstrand crosslinks. *Nucleic Acids Res.* 23, 42-50.

(10) APPENDICES:

Manuscript published acknowledging support:

Podell, E. R.; Harrington, D. J.; Taatjes, D. J.; Koch, T. H. "Crystal Structure of Epidoxoform-formaldehyde *Virtual Crosslink* of DNA and Evidence for Its Formation in Human Breast Cancer Cells" *Acta Cryst., D55*, 1516-1523 (1999).

research papers

Crystal structure of epidoxorubicin–formaldehyde virtual crosslink of DNA and evidence for its formation in human breast-cancer cells

Elaine R. Podell,[a,b] Daniel J. Harrington,[a,b] Dylan J. Taatjes[a] and Tad H. Koch[a,c]*

[a]Department of Chemistry and Biochemistry, University of Colorado, Boulder, Colorado 80309-0215, USA, [b]Howard Hughes Medical Institute, University of Colorado, Boulder, Colorado 80309-0215, USA, and [c]University of Colorado Cancer Center, Denver, CO 80262, USA

Correspondence e-mail:
tad.koch@colorado.edu

Epidoxorubicin and daunorubicin are proposed to be cytotoxic to tumor cells by catalyzing production of formaldehyde through redox cycling and using the formaldehyde for covalent attachment to DNA at G bases. The crystal structure of epidoxorubicin covalently bound to a d(CGCGCG) oligomer was determined to 1.6 Å resolution. The structure reveals slightly distorted B-form DNA bearing two molecules of epidoxorubicin symmetrically intercalated at the termini, with each covalently attached from its N3' to N2 of a G base *via* a CH$_2$ group from the formaldehyde. The structure is analogous to daunorubicin covalently bound to d(CGCGCG) determined previously, except for additional hydrogen bonding from the epimeric O4' to O2 of a C base. The role of drug–DNA covalent bonding in cells was investigated with synthetic epidoxorubicin–formaldehyde conjugate (Epidoxoform) and synthetic daunorubicin–formaldehyde conjugate (Daunoform). Uptake and location of drug fluorophore in doxorubicin-resistant human breast-cancer cells (MCF-7/ADR cells) was observed by fluorescence microscopy and flow cytometry. The fluorophore of Daunoform appeared more rapidly in cells and was released more rapidly from cells than the fluorophore of Epidoxoform over a 3 h exposure period. The fluorophore appeared predominantly in the nucleus of cells treated with both conjugates. The difference in uptake is explained in terms of the slower rate of hydrolysis of Epidoxoform to the species reactive with DNA and a proposed slower release from DNA based upon the crystal structures.

1. Introduction

Epidoxorubicin, the 4'-epimer of the clinically important antitumor drug doxorubicin, is a broad-spectrum anthracycline antitumor drug approved for human use in all countries of the world except the USA. A third relevant anthracycline, daunorubicin, is identical to doxorubicin except for the absence of the 14-hydroxyl group. Recent experiments by us and others indicate that all three of these anthracyclines derive at least some, if not most, of their antitumor activity through induction of oxidative stress leading to formaldehyde production. The drugs bind the formaldehyde at their 3'-amino substituents and use this formaldehyde moiety for covalent attachment to DNA at the 2-amino substituents of G bases (Cullinane, Cutts *et al.*, 1994; Cullinane, van Rosmalen *et al.*, 1994; Cutts *et al.*, 1996; Cutts & Phillips, 1995; Taatjes, Fenick, Gaudiano *et al.*, 1998; Taatjes, Gaudiano & Koch, 1997; Taatjes, Gaudiano, Resing *et al.*, 1997; Taatjes *et al.*, 1996; Wang *et al.*, 1991). The crystal structure of daunorubicin covalently attached to the self-complementary DNA oligomer

d(CGCGCG) *via* formaldehyde was solved even before drug-induced formaldehyde production was discovered (Wang *et al.*, 1991), and the structure was important in the elucidation of the mechanism. The drug–DNA covalent-binding mechanism then led to the synthesis of daunorubicin–, doxorubicin– and epidoxorubicin–formaldehyde conjugates, Daunoform (DAUF), Doxoform (DOXF) and Epidoxoform (EPIF), respectively, as improved antitumor drugs (Fenick *et al.*, 1997; Taatjes, Fenick & Koch, 1998). Of particular importance is that the conjugates are significantly more active against resistant cancer cells than the corresponding clinical drugs (Fenick *et al.*, 1997; Taatjes, Fenick & Koch, 1998). In each case, the formaldehyde conjugate is proposed to be a prodrug of the active metabolite of the clinical drug, with the metabolite released through partial hydrolysis of the conjugate. Structures for the clinical drugs, the formaldehyde conjugates and the active metabolites are shown in Fig. 1.

Of the three conjugates, Epidoxoform has emerged as the lead structure for further development because it is hydrolytically more stable with respect to release of formaldehyde (Fenick *et al.*, 1997; Taatjes, Fenick & Koch, 1998). Consequently, Epidoxoform or the product of its partial hydrolysis has a longer potential residence time in the vascular system. On this basis, the crystal structure of epidoxorubicin covalently attached to d(CGCGCG) *via* formaldehyde was solved and is reported here. The structure is compared with that of daunorubicin covalently attached to d(CGCGCG) (Wang *et al.*, 1991) and the structure of epidoxorubicin intercalated in d(CGATCG) (Williams *et al.*, 1990). Both structures are discussed in terms of uptake of Epidoxoform and Daunoform by resistant breast-cancer cells.

2. Materials and methods

2.1. Materials

All tissue-culture materials were obtained from Gibco Life Technologies (Grand Island, NY) unless otherwise stated. MCF-7/ADR breast-cancer cells were a gift from Dr William W. Wells (Michigan State University). Daunoform (DAUF) and Epidoxoform (EPIF) were synthesized from daunorubicin and epidoxorubicin, respectively, by reaction with formaldehyde, as described previously (Fenick *et al.*, 1997; Taatjes, Fenick & Koch, 1998). DAPI (4,6-diamidino-2-phenylindole), spermine and sodium cacodylate were from Sigma Chemical Co. DNA oligonucleotide was obtained from Integrated DNA Technologies (Coralville, IA) and purified by reverse-phase HPLC as described previously (Taatjes, Guadiano, Resing *et al.*, 1997). Formaldehyde was obtained from Mallinckrodt as a 37%(w/w) solution in water containing 10–15% methanol; barium chloride was obtained from Fisher Chemical Co.; 2-methyl-2,4-pentanediol (MPD) was from Aldrich Chemical Co. Water was distilled and purified with a Millipore Q-UF Plus purification system to 18 MΩ cm.

2.2. X-ray crystallography

Crystallization trials were based upon conditions described for daunorubicin–CH$_2$–d(CGCGCG) (Wang *et al.*, 1991). The crystallization mixture consisted of 1.2 mM d(CGCGCG), 1.2 mM epidoxorubicin and 9 mM formaldehyde in pH 6.0 buffer containing 30 mM sodium cacodylate, 16.1 mM spermine and 4.4 mM BaCl$_2$. Tetragonal crystals were grown in sterile 24-well plates (ICN Biomedicals, Aurora, OH) by the hanging-drop method on silanized cover slips. A 4 µl drop of
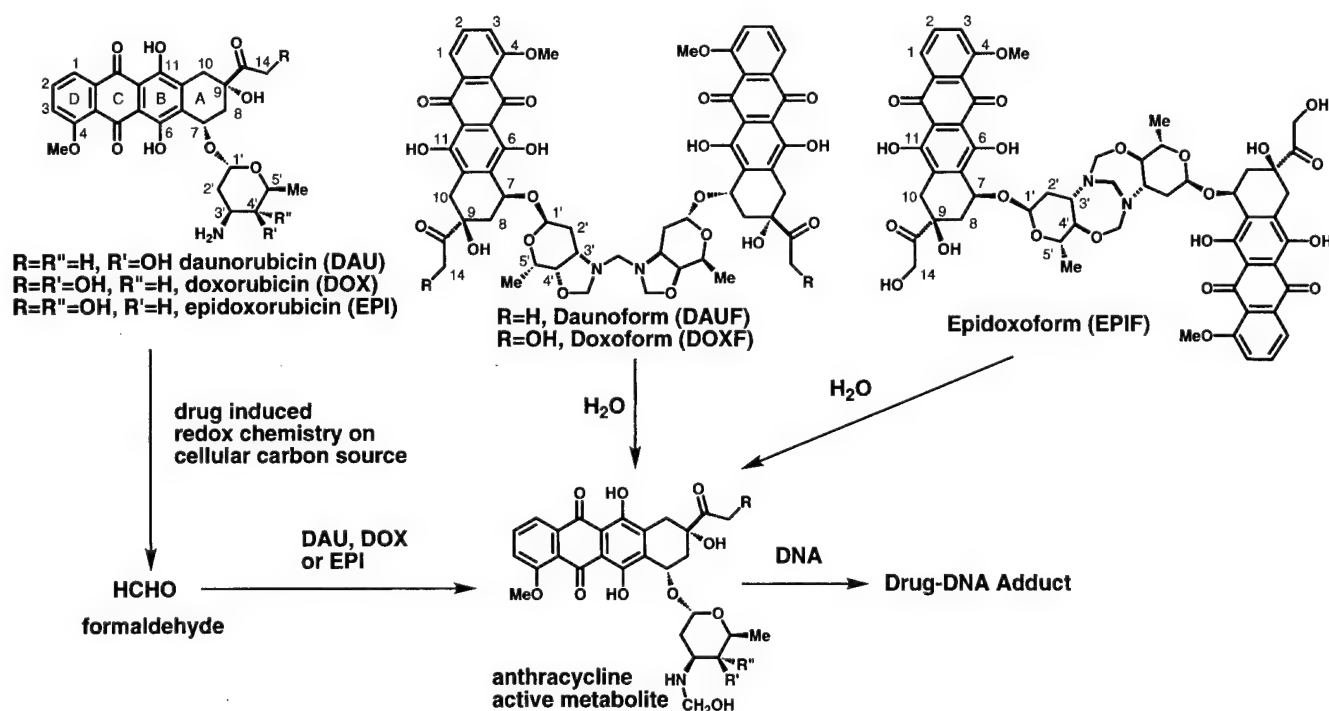
Figure 1
Structures of clinical anthracycline antitumor drugs, their metabolites and their conjugates with formaldehyde.

Table 1
Crystallographic parameters.

Data-collection and refinement statistics.

Unit-cell dimensions (Å, °)	$a = 28.11$, $b = 28.11$, $c = 52.54$; $\alpha = 90$, $\beta = 90$, $\gamma = 90$
Space group	$P4_12_12$
Temperature (K)	295
Number of collected reflections to 1.6 Å	47174
Number of unique reflections to 1.6 Å	3101
Number of reflections used for refinement [$F > 2\sigma(F)$]	2054†, 2612‡
R_{sym}§ (%)	9.9
R factor (%)	20.52†, 21.64‡
R_{free} (%)	26.78†
R.m.s. deviation of bonds from ideality (Å)	0.0197
R.m.s. deviation of angles from ideality (°)	2.087
Average B value (Å^2)	19.37
Number of observed solvent molecules	30
Overdeterminacy ratio	2.9†, 3.7‡

Number of reflections, R_{sym} and completeness by resolution.

Resolution range (Å)	No. of reflections	R_{sym} (%)	Completeness (%)
99.0–3.45	338	7.5	90.0
3.45–2.74	302	9.2	95.0
2.74–2.39	303	11.1	96.2
2.39–2.17	287	12.1	94.1
2.17–2.02	285	13.4	94.4
2.02–1.90	281	14.3	92.1
1.90–1.80	272	18.4	92.5
1.80–1.72	282	22.8	92.5
1.72–1.66	256	26.8	89.8
1.66–1.60	2482	30.9	82.7
All hkl	2854	9.9	92.0

† After sequestering 17.3% of the data. ‡ With all the data. § $R_{sym} = \sum[Abs(I - \langle I \rangle)]/\sum I$.

the crystallization mixture was placed on a cover slip and the drop was sealed over a 1 ml well solution containing 40% MPD in water. Crystals were allowed to grow at ambient temperature; crystal formation was complete in about 6 d. The crystal was mounted and sealed in a glass capillary tube, and diffraction data were collected on an R-AXIS II image-plate system using Cu $K\alpha$ radiation from a Rigaku RU-H2R rotating-anode X-ray generator (Molecular Structures Corp., Houston, TX). The data were reduced and scaled using the *HKL* package (Gewirth, 1997; Otwinowski & Minor, 1997) and are summarized in Table 1. Epidoxorubicin–CH$_2$–d(CGCGCG) crystals belong to the space group $P4_12_12$, like many anthracycline–hexanucleotide complexes, and have unit-cell parameters $a = b = 28.11$, $c = 52.54$ Å, $\alpha = \beta = \gamma = 90°$. Useful diffraction was seen to a minimum Bragg spacing of 1.6 Å.

Crystallographic refinement and σ_A-weighted electron-density map calculations were carried out using *CNS* (Brünger *et al.*, 1998), with a new parameter dictionary for standard DNA nucleotides (Parkinson *et al.*, 1996). The initial model was constructed from the coordinates of daunorubicin covalently linked to d(CGCGCG) with formaldehyde (PDB entry 1d33) modified to include the position of O14 from epidoxorubicin (PDB entry 1d54). All refinement was performed on

$|F_o| > 2\sigma|F_o|$. In order to obtain a statistically significant set of reflections for R_{free} calculations (Brünger & Rice, 1997), 529 reflections (17.3%) were sequestered from the data set. Initial refinement used the R_{free}, while the final series of conjugate-gradient minimizations utilized the entire data set in order to include a significant percentage (84.5%) of the theoretical data to 1.6 Å. The first set of refinement rounds consisted of torsion-angle simulated annealing with the maximum-likelihood target using amplitudes as implemented in *CNS*, followed by cycles of water picking based on positive peaks in $F_o - F_c$ difference Fourier maps. After each cycle of water picking, conjugate-gradient minimization and individual temperature-factor refinement was carried out and water positions were checked by examining $2F_o - F_c$ and $F_o - F_c$ difference Fourier maps calculated by *CNS* and displayed on a Silicon Graphics Onyx 2 workstation using *O* (Jones *et al.*, 1991). After 29 waters were picked, the model was annealed again and the cycles continued with some waters being manually repositioned into density as necessary. In the last cycle, waters with temperature factors greater than 60 Å^2 were deleted. In the final series of refinement cycles, the model was refined against all reflections using the standard crystallographic residual target and a bulk-solvent correction. As in the first set, cycles of conjugate-gradient minimization and individual temperature-factor refinement were performed, followed by scrutinizing the $F_o - F_c$ and $2F_o - F_c$ maps. Additional waters were deleted or repositioned based on the same criteria of lower temperature factors and occupied density. No other ions (Na$^+$, spermine or Ba^{2+}) could be unambiguously identified. The final model contained 30 waters distributed throughout the epidoxorubicin–CH$_2$–d(CGCGCG) asymmetric unit. Crystallographic and refinement data are reported in Table 1.

2.3. Measurement of drug uptake by flow cytometry

MCF-7/ADR cells were maintained *in vitro* by serial culture in RPMI 1640 medium supplemented with 10% fetal bovine serum (Gemini Bio-Products, Calbasas, CA), L-glutamine (2 mM), HEPES buffer (10 mM), penicillin (100 units ml^{-1}), streptomycin (100 mg ml^{-1}) and 5 µM doxorubicin. Cells were maintained at 310 K in a humidified atmosphere of 5% CO$_2$ and 95% air. Cultured cells were dissociated with trypsin–EDTA and plated in 6-well plates (∼500000 cells per well) and allowed to adhere overnight. The cells were treated with 0.25 µM DAUF or EPIF at 310 K for various amounts of time (5 min, 30 min, 1 h, 2 h, 3 h). For each time point, the medium was removed and the cells were trypsinized and suspended in 3 ml of RPMI 1640 medium (−) phenol red and (−) FBS. The cells were transferred to 15 ml conical vials and centrifuged at 1000 r min^{-1} for 5 min at 283 K. The supernatant was removed and replaced with 1 ml of RPMI 1640 medium (−) phenol red and (−) FBS. The cells were kept at 273 K until analysis (up to 3 h). Control experiments showed no significant loss of fluorescence in samples kept at 273 K for up to 4 h. The extent of drug uptake was determined by flow cytometry, as previously described (Durand & Olive, 1981). All flow-

cytometry measurements were made with a Becton Dickinson FACScan flow cytometer, using a Hewlett–Packard 9000 Series Model 340 computer for data storage and analysis. Drug-treated cells were analyzed with excitation at 488 nm (15 mW argon-ion laser), with emission monitored between 570 and 600 nm. Instrument settings were held constant for all experiments and 5000 cells were counted per measurement. The emission of drug-free cells was similarly measured in order to determine background fluorescence. The final data are plotted as mean fluorescence (as determined by computer data analysis) *versus* drug incubation time (or recovery time) for ease of data representation.

2.4. Analysis of intracellular drug distribution by fluorescence microscopy

Cells were plated in 6-well plates (~300 000 cells per well). Each well contained a sterile cover slip, and the cells were allowed to adhere to the cover slip overnight. Each well contained 3 ml of RPMI 1640 medium. The DAUF and EPIF were dissolved in DMSO to a concentration of 25 μM (100× solution). 30 μl of each DMSO solution was then added to the appropriate well, resulting in a 100× dilution (0.25 μM conjugate, 1% DMSO). The cells were incubated with the drug for 3 h. Following drug treatment, the medium was removed and the cells were washed with 2 ml PBS (phosphate-buffered saline). The cells were then fixed to the cover slips by submerging in 3 ml cold (253 K) methanol and storing on ice for 5 min. The methanol was then removed and the cells were washed with 3 ml PBS. The cover slips were then removed from the wells and inverted on a drop (30 μl) of DAPI (0.2 μg ml^{-1} in PBS) placed on parafilm. The cover slips were kept on the DAPI solution for 5 min at ambient temperature. The cover slips were then rinsed with PBS and mounted on a microscope slide using a drop (30 μl) of mowiol mounting medium. The slides were allowed to dry in the dark overnight. Microscopic images were observed at a magnification of 1000× and recorded with a Zeiss Axioplan fluorescence microscope equipped with a Photometrics Sensys digital CCD camera system. Images were manipulated using *IP-LAB Spectrum* software. Drug fluorescence in cells was observed at wavelengths longer than 590 nm with excitation at 546 ± 6 nm. DAPI fluorescence was observed at wavelengths longer than 420 nm with excitation at 355 ± 20 nm.

3. Results and discussion

3.1. Crystal structure of epidoxorubicin covalently bound to d(CGCGCG)

The crystallographic asymmetric unit consists of a single strand of d(CGCGCG) covalently attached to a 4′-epidoxorubicin molecule *via* a methylene group at one of the guanines and 30 ordered water molecules. Two asymmetric units form a slightly distorted B-type DNA duplex with six Watson–Crick base pairs. Fig. 2 shows [4′-epidoxorubicin–CH$_2$–d(CGCGCG)]$_2$ with the DNA displayed as a CPK structure and the drug as a framework structure. As observed in other anthracycline–DNA structures, the aglycon rings of epidoxorubicin are intercalated at CpG steps, with the D ring reaching into the major groove while the sugar moiety lies in the minor groove. The intercalation sites are C(1)G(2)/G(12)C(11) and C(5)G(6)/G(8)C(7). [The nucleotides labeled C(1)–G(6) are on a strand in one asymmetric unit, with C(7)–G(12) located on the complementary strand generated by twofold crystallographic symmetry]. Two methylene groups link the 3′-amino substituents of two epidoxorubicins to the 2-amino substituents of G(10) and G(4). Fig. 3 shows a stereoscopic view of the $F_o - F_c$ electron-density map superimposed on the final model of 4′-epidoxorubicin–CH$_2$–d(CGCGCG).

Comparison of the structure with the covalent daunorubicin–CH$_2$–d(CGCGCG) (Wang *et al.*, 1991) and the non-covalent 4′-epidoxorubicin–d(CGATCG) structures (Williams *et al.*, 1990) is instructive and is summarized in Table 2 and Fig. 4. The general coordinate error based on the Luzzati plot for our model is 0.20 Å. Of particular significance are hydrogen-bonding interactions between the drug and the DNA. The O9 hydroxyl groups of the drugs in all three structures are hydrogen bonded to N2 and N3 of G(8) with approximately the same bond distances (3.12–3.15 and 2.89–2.59 Å, respectively). The
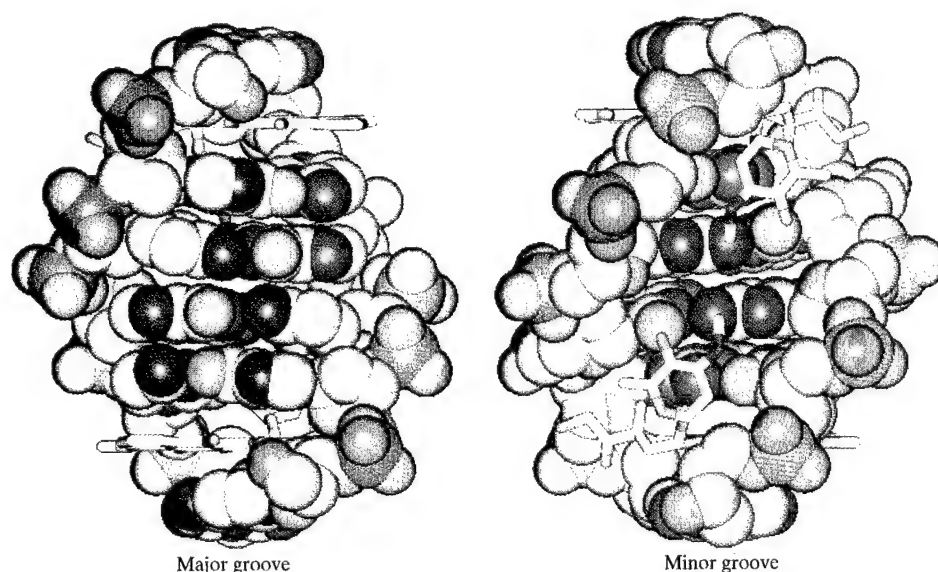
Figure 2
Epidoxorubicin–CH$_2$–d(CGCGCG), with DNA displayed as a CPK structure and epidoxorubicin–CH$_2$ displayed as a framework structure. This figure was created with *Insight*II (Biosym Technologies, San Diego, CA).

Table 2
Distances.

Drug atom	DNA atom	Water atom†	Epidox–CH₂–d(CG)₃‡	Dauno–CH₂–d(CG)₃	Epidox–d(CGATCG)
O9	G(8) N3		2.89	2.86	2.59
	G(8) N2		3.12	3.12	3.15
O7	G(8) N2		2.87	3.13	3.35
O14	C(9) C5′		3.70	—	—
	A(9) C5′		—	—	3.40
O4′	C(9) O2		2.70	>4.0	—
	A(9) N3		—	—	3.06
N3′	G(4) N2		2.50	2.48	—
	T(4) O2		—	—	3.37
	C(5) O2		3.33	3.24	3.27
	C(5) O4′		3.55	3.16	3.31
	CH₂		1.52	1.53	—
CH₂	G(4) N2		1.46	1.45	—
O4		W(1)	2.81	3.06	3.02
O5		W(1)	3.02	3.21	3.11
	G(6) N7	W(1)	2.69	2.72	2.83
O12		W(25)	2.90	3.81	>4.0
	G(8) N7	W(25)	3.07	3.01	2.61
O13		W(6)	2.89	3.11	3.34
	C(7) O2	W(6)	2.84	2.60	2.65

† Naming convention from epidoxorubicin–CH₂–d(CGCGCG) structure. ‡ Luzzati coordinate error = 0.20 Å.

distance between the anomeric O7 of the drug and the N2 of G(8) is shorter in epidoxorubicin–CH₂–d(CGCGCG) than in the other structures (2.87 *versus* 3.13 and 3.35 Å), suggesting that there is a stronger hydrogen bond between these atoms. The primary structural difference between epidoxorubicin and daunorubicin is the configuration of the hydroxyl at the 4′-position. This leads to a good hydrogen-bonding interaction (2.70 Å) with the O2 of C(9) on the complementary strand in the structure of epidoxorubicin–CH₂–d(CGCGCG). In epidoxorubicin–d(CGATCG), this hydrogen bonding is with the N3 of the adenine on the complementary strand. Perhaps the extra hydrogen bonding causes the aglycon A ring of the drug to lie closer to G(8) on the complementary strand in epidoxorubicin–CH₂–d(CGCGCG). The 14-hydroxyl, present
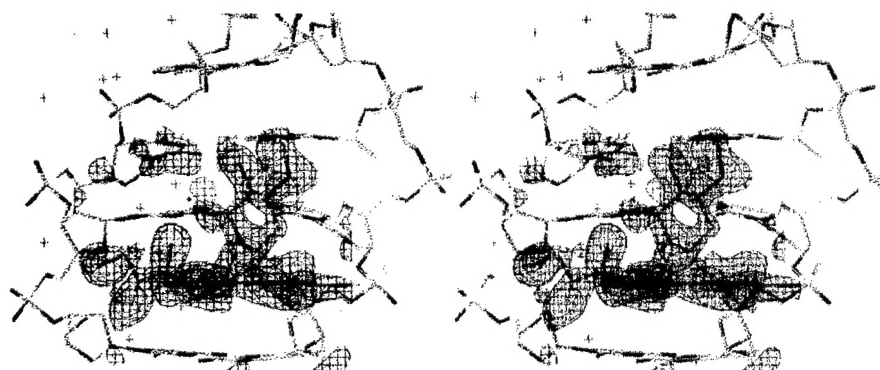
in the epidoxorubicin structures but not in the daunorubicin structure, lies farther away from the C5′ of C(9) on the complementary strand in the covalent structure than in the non-covalent structure (3.70 *versus* 3.40 Å). Differences in the A ring, O7, O14 and aminosugar of the drugs in the three structures are shown *via* an overlay diagram in Fig. 5. The alignment was performed using all the common atoms, including the atoms of the nucleic acid moieties, between epidoxorubicin–CH₂–d(CGCGCG) as the reference molecule and either daunorubicin–CH₂–d(CGCGCG) or epidoxorubicin–d(CGATCG). For clarity, the superimposed DNA from the structures was omitted from Fig. 5. The O12 is within hydrogen-bonding distance (2.90 Å) of a water molecule, W(25), which is associated with the N7 of guanine G(8) (3.07 Å). [Solvent water molecules are labeled W(1)–W(30).] While the other two structures also have a water molecule near N7 of G(8) (3.01 or 2.61 Å), it is too far away from O12 (3.81 or >4.01 Å) to mediate contact between the drug and the DNA. All of these drug–DNA and drug–water molecule contacts are summarized in Table 2 and Fig. 4.

The drug–DNA adducts are hydrolytically unstable, and the drug is released at two different first-order rates, one with a half-life of 5 h and the other of 40 h (Cullinane, van Rosmalen *et al.*, 1994; van Rosmalen *et al.*, 1995). Prior to an understanding of the molecular nature of the covalent bonding, the drug released more slowly was thought to be covalently attached to both strands of the DNA at the G bases of a GC site. The crystal structure reported here and the earlier structure of daunorubicin covalently bound to d(CGCGCG) (Wang *et al.*, 1991) provide a simple explanation for slower release of drug from a GC site, even though the drug has only one covalent attachment. In addition to the covalent attachment to a G on one strand, the drug is strongly hydrogen bonded between its 9-hydroxyl and the N atoms at the 2- and 3-positions of the guanine on the complementary strand. The [epidoxorubicin–CH₂–d(CGCGCG)]₂ structure also suggests hydrogen bonding between O7 of the drug and N2 of G(8) and between O4′ of the drug and O2 of C(9) on the complementary strand. Because the original proposal for the structure of more stable lesions was thought to be a crosslink of DNA by the drug, we proposed the term virtual crosslink for this bonding, which is unique to the GC dinucleotide. The less stable DNA–drug adducts are then proposed to have covalent attachment to isolated G bases *via* methylene groups, and to be missing the hydrogen-bonding interactions with the opposing strand.

The virtual crosslink of the self-complementary hexanucleotide d(ATGCAT) at the TGC site from reaction with a single doxorubicin and formaldehyde has recently been characterized using NMR spectroscopy (Zeman *et al.*, 1998). This study also reported the effect of the virtual cross-

Figure 3
Stereoscopic view of an $F_o - F_c$ electron-density map superimposed on the final model of epidoxorubicin–CH₂–d(CGCGCG). All atoms of the drug were omitted during the map calculation using only the coordinates in the final model of the DNA molecule for the phase information. The density is contoured at 2σ. Bonds and atoms are colored according to atom type.

link on the stability of duplex DNA from measurements of the rate of DNA-strand exchange. Strand exchange was 3.9 times slower with a doxorubicin merely intercalating in an oligo-nucleotide but 637 times slower with a doxorubicin virtually crosslinking the oligonucleotide.

3.2. Uptake and distribution of drug in MCF-7/ADR cells

MCF-7/ADR cells are mutants of the MCF-7 human breast-cancer cell line which are highly resistant to doxorubicin (Adriamycin). They are also resistant to daunorubicin and epidoxorubicin but not to Daunoform, Epidoxoform or Doxoform (Fenick et al., 1997; Taatjes, Fenick & Koch, 1998). Important resistance mechanisms are increased activity of enzymes which neutralize the effects of drug-induced oxidative stress and overexpression of the drug efflux pump, P-170 glycoprotein (Pgp) (Mimnaugh et al., 1991; Sinha & Mimnaugh, 1990). This cell line, therefore, is particularly useful for studying the effect of the conjugation of the drug with formaldehyde, because daunorubicin and epidoxorubicin are maintained at lower concentrations by drug efflux. The efflux pump recognizes the drugs partly because of the positive charge at the amino substitutent (Lampidis et al., 1997). Formaldehyde conjugates are uncharged because of a change in pK_a resulting from the hydroxymethylene substituent and hence are predicted to be poorer substrates for Pgp. Further, formation of active metabolite by the clinical drug is enzymatically inhibited in MCF-7/ADR cells.

Uptake of Daunoform and Epidoxoform by MCF-7/ADR cells at 310 K as a function of time of exposure to 0.25 μM drug was measured by flow cytometry (Fig. 6). Drug fluorophore in cells was detected by its fluorescence in the region of 590 nm. The fluorophore in cells treated with Daunoform appeared rapidly, with the maximum level occurring after approximately 7 min, followed by a steady decrease during the

remaining 3 h exposure period. In contrast, fluorophore in cells treated with Epidoxoform steadily increased over the 3 h exposure period. The rates of uptake parallel the rates of hydrolysis of conjugates to the active metabolites of the respective clinical drugs (Fig. 1). Hydrolysis of Daunoform to the active metabolite occurs with a half-life of less than 10 min in cell-culture medium at 298 K (Fenick et al., 1997), while hydrolysis of Epidoxoform to the active metabolite occurs with a half-life of 2 h at 310 K in cell-culture medium (Taatjes, Fenick & Koch, 1998). Further, the half-lives for hydrolysis of the active metabolites to daunorubicin and epidoxorubicin are less than 10 min and greater than 2 h, respectively. This parallel suggests that the slow step for drug uptake by MCF-7/ADR cells is hydrolysis to the active metabolite.

The location of drug fluorophore in the nucleus of MCF-7/ADR cells treated with either Daunoform or Epidoxoform was established by fluorescence microscopy, as shown in Fig. 6. Anthracycline fluorescence was primarily in the nucleus, as indicated by co-staining with the nuclear stain DAPI. The abundance of anthracycline in the nucleus is even higher than indicated by the micrographs because DNA partially quenches the fluorescence (Crooke & DuVernay, 1980; Roche et al., 1994). Since the anthracycline is predominantly in the nucleus, the release of fluorophore from cells exposed to Daunoform after 7 min of drug treatment can be explained by hydrolysis of drug covalently bound to DNA occurring faster than new covalent binding of drug metabolite. In fact, after about 30 min most of the Daunoform in the cell-culture medium has hydrolyzed to daunorubicin, which is not significantly taken up by MCF-7/ADR cells because of the Pgp efflux pump. Further, formation of the active metabolite from daunorubicin is inhibited in these cells by the increased activity of enzymes which neutralize oxidative stress. The rate of fluorophore release over the 3 h time period is most consistent with predominant hydrolysis of drug–DNA lesions at isolated G bases. This hydrolysis releases daunorubicin which is pumped out of the cell. Steady increase of fluorophore in MCF-7/ADR cells upon treatment with Epidoxoform over the 3 h time period is a consequence of much slower
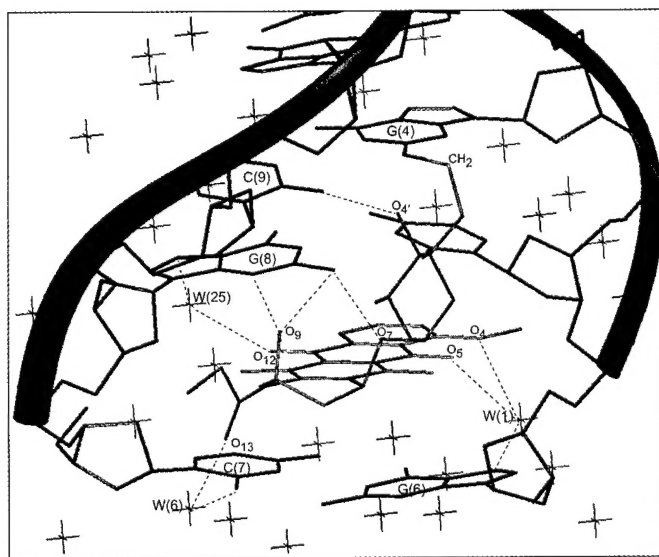
Figure 4
Hydrogen-bonding contacts between epidoxorubicin–CH$_2$ and d(CGCGCG). This figure was created with InsightII (Biosym Technologies, San Diego, CA).
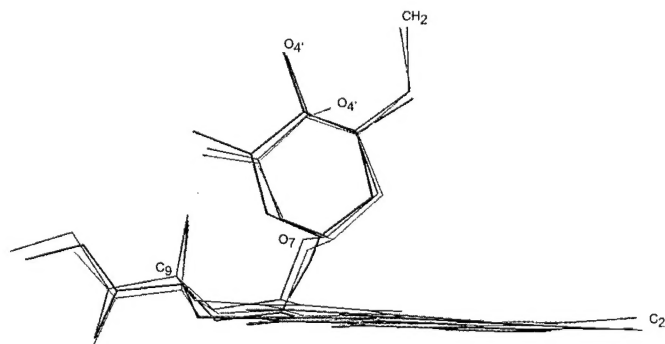
Figure 5
Overlay of epidoxorubicin (in black) and daunorubicin–CH$_2$ (in green) on epidoxorubicin–CH$_2$ (in red). R.m.s.d. in distance of all atoms common to epidoxorubicin–CH$_2$–d(CGCGCG) and daunorubicin–CH$_2$–d(CGCGCG) is 0.923 Å and between epidoxorubicin–CH$_2$–d(CGCGCG) and epidoxorubicin–d(CGATCG) is 0.829 Å. For clarity, the overlaid DNA strands have been omitted from the figure.

hydrolysis to the active metabolite and increased stability of the metabolite with respect to further hydrolysis to epidoxorubicin. Hence, covalent bonding of drug to DNA is occurring faster than hydrolysis of drug–DNA lesions. Additional evidence for covalent binding of drug to DNA in cells comes from a comparison of release of drug from cells treated with

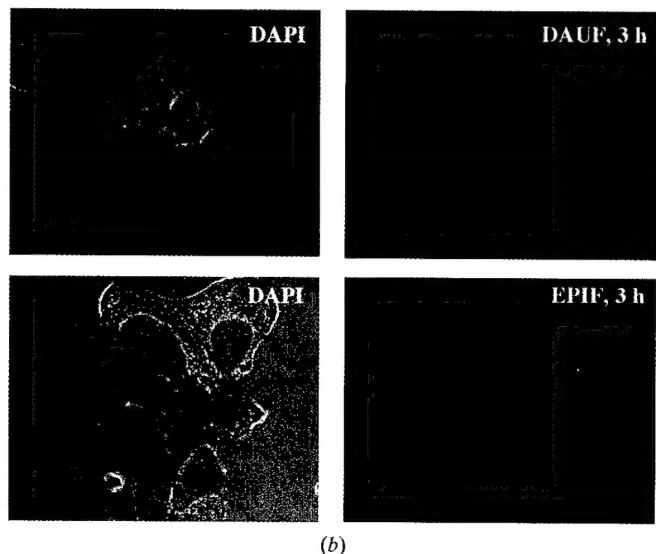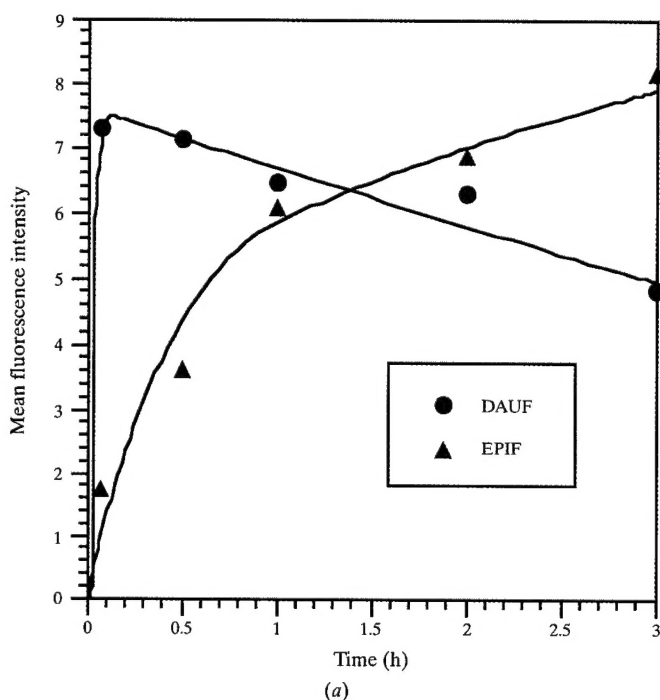either parent drug or formaldehyde conjugate and from analysis of cells treated with tritiated formaldehyde conjugate (Taatjes *et al.*, 1999).

The crystal structure provides some additional insight with respect to drug uptake by MCF-7/ADR cells. The additional hydrogen-bonding interaction between the epidoxorubicin's 4′-hydroxyl and the O2 of C(9) on the complementary strand should lead to slower hydrolysis of the virtual crosslink of DNA with epidoxorubicin than with daunorubicin. This slower release from DNA gives rise to continued uptake as Epidoxoform is slowly hydrolyzing to the active metabolite. Daunoform hydrolyzes to its active metabolite very rapidly, which causes a rapid buildup of drug in the nucleus of tumor cells. The intracellular levels then also decrease because of the predicted less stable daunorubicin virtual crosslink.

In summary, the 1.6 Å crystal structure of [epidoxorubicin–CH_2–d(CGCGCG)]$_2$ shows a slightly distorted B-type DNA duplex symmetrically bearing two intercalated epidoxorubicin molecules located at the termini which are covalently attached to the DNA *via* methylene groups. Covalent attachment is from the 3′-amino group of epidoxorubicin to the 2-amino group of G(4) or G(10). The structure is analogous to the structure of [daunorubicin–CH_2–d(CGCGCG)]$_2$, except for additional hydrogen bonding from the 4′-hydroxyl group of epidoxorubicin to the O2 of C(3) or C(9). This hydrogen bonding, together with hydrogen bonding between O7 and O9 of the drug and N2 and/or N3 of G(2) or G(8) and the covalent attachment, result in a virtual crosslinking of DNA by drug. Flow cytometry and fluorescence microscopy show that daunorubicin–formaldehyde conjugate (Daunoform) and epidoxorubicin–formaldehyde conjugate (Epidoxoform) are readily taken up by doxorubicin-resistant human breast-cancer cells and locate predominantly in the nucleus. Differences in the rates of uptake are consistent with differences in the rates of hydrolysis of the conjugates to the proposed DNA-reactive form of the drugs and differences in the respective structures of the drugs covalently bound to DNA.

Figure 6
(*a*) Uptake of the fluorophore of Daunoform (DAUF) or Epidoxoform (EPIF) by MCF-7/ADR cells as a function of time of exposure to 0.25 μ*M* drug, as determined by flow cytometry measuring fluorescence intensity at 570–600 nm. (*b*) Fluorescence micrographs of MCF-7/ADR cells after treatment with either 0.25 μ*M* Daunoform or Epidoxoform for 3 h. After drug treatment, cells were fixed and stained with the nuclear stain DAPI. Each micrograph showing DAPI fluorescence in green superimposed on the whole cell image is located adjacent to the respective micrograph showing drug fluorophore emission.

References

Brünger, A. T., Adams, P. D., Clore, G. M., Delano, W. L., Gros, P., Grosse-Kunstleve, R. W., Fiang, J., Kuszewski, J., Niles, M., Pannu, N. S., Read, R. J., Rice, L. M., Simmonson, T. & Warren, G. L. (1998). *Acta Cryst.* D**54**, 905–921.

Brünger, A. T. & Rice, L. M. (1997). *Methods Enzymol.* **277**, 243–269.

Crooke, S. T. & DuVernay, V. H. (1980). *Anthracyclines: Current Status and New Developments*, edited by S. T. Crooke & S. D. Reich, pp. 151–155. New York: Academic Press.

Cullinane, C., Cutts, S. M., van Rosmalen, A. & Phillips, D. R. (1994). *Nucleic Acids Res.* **22**, 2296–2303.

Cullinane, C., van Rosmalen, A. & Phillips, D. R. (1994). *Biochemistry*, **33**, 4632–4638.

Cutts, S. M., Parsons, P. G., Sturm, R. A. & Phillips, D. R. (1996). *J. Biol. Chem.* **271**, 5422–5429.

Cutts, S. M. & Phillips, D. R. (1995). *Nucleic Acids Res.* **23**, 2450–2456.

Durand, R. E. & Olive, P. L. (1981). *Cancer Res.* **41**, 3489–3494.

Fenick, D. J., Taatjes, D. J. & Koch, T. H. (1997). *J. Med. Chem.* **40**, 2452–2461.

Gewirth, D. (1997). *The HKL Manual – A Description of Programs DENZO, XDISPLAYF and SCALEPACK*, 5th ed. New Haven, CT: Yale University Press.

Jones, T. A., Zou, J. Y., Cowan, S. W. & Kjeldgaard, M. (1991). *Acta Cryst.* A**47**, 110–119.

Lampidis, T. J., Kolonias, D., Podona, T., Israel, M., Safa, A. R., Lothstein, L., Savaraj, N., Tapiero, H. & Priebe, W. (1997). *Biochemistry*, **36**, 2679–2685.

Mimnaugh, E. G., Fairchild, C. R., Fruehauf, J. P. & Sinha, B. K. (1991). *Biochem. Pharmacol.* **42**, 391–402.

Otwinowski, Z. & Minor, W. (1997). *Methods Enzymol.* **276**, 307–326.

Parkinson, G., Vojtechovshy, J., Clowney, L., Brünger, A. T. & Berman, H. M. (1996). *Acta Cryst.* D**52**, 57–64.

Roche, C. J., Thomson, J. A. & Crothers, D. M. (1994). *Biochemistry*, **33**, 926–935.

Rosmalen, A. van, Cullinane, C., Cutts, S. M. & Phillips, D. R. (1995). *Nucleic Acids Res.* **23**, 42–50.

Sinha, B. K. & Mimnaugh, E. G. (1990). *Free Rad. Biol. Med.* **8**, 567–581.

Taatjes, D. J., Fenick, D. J., Gaudiano, G. & Koch, T. H. (1998). *Curr. Pharm. Des.* **4**, 203–218.

Taatjes, D. J., Fenick, D. J. & Koch, T. H. (1998). *J. Med. Chem.* **41**, 2452–2461.

Taatjes, D. J., Fenick, D. J. & Koch, T. H. (1999). *Chem. Res. Toxicol.* **12**, 588–596.

Taatjes, D. J., Gaudiano, G. & Koch, T. H. (1997). *Chem. Res. Toxicol.* **10**, 953–961.

Taatjes, D. J., Gaudiano, G., Resing, K. & Koch, T. H. (1996). *J. Med. Chem.* **39**, 4135–4138.

Taatjes, D. J., Gaudiano, G., Resing, K. & Koch, T. H. (1997). *J. Med. Chem.* **40**, 1276–1286.

Wang, A. H. J., Gao, Y. G., Liaw, Y. C. & Li, Y. K. (1991). *Biochemistry*, **30**, 3812–3815.

Williams, L. D., Frederick, C. A., Ughetto, G. & Rich, A. (1990). *Nucleic Acids Res.* **18**, 5533–5541.

Zeman, S. M., Phillips, D. R. & Crothers, D. M. (1998). *Proc. Natl Acad. Sci. USA*, **95**, 11561–11565.